Computer Fraud and Security
ISSN (online): 1873-7056

State Perception and Health Prediction of Key Equipment in Power Metering Production

Chong Li, Hongtao Shen, Juchuan Guo*, Hongming Ma, Yi Wang, Rongkun Guo
State Grid Hebei Markting Service Center, Shijiazhuang 050000, Hebei, China
**Corresponding Author.*

Abstract:
Combining intelligent sensing technology with an improved grey wolf optimizer (GWO) algorithm, this article innovatively studied state perception and health prediction methods for key power metering equipment. A state perception network was constructed, utilizing intelligent sensing for real-time collection and monitoring of equipment operation. Gabor transform was applied for signal denoising, followed by empirical mode decomposition to extract operational features. An improved GWO algorithm enhanced search efficiency and global optimization, avoiding local optima. A combination prediction model was established to improve prediction accuracy and reliability. Results showed average data collection and processing times of 0.053 and 0.196 seconds, with 93.84% accuracy, and fault warning and false alarm rates of 93.37% and 6.63%, respectively. This method effectively monitors equipment state and predicts health, aiding proactive maintenance planning and reducing fault costs.

Keywords: power metering production, health prediction, state perception network, feature signal extraction, internet of things and machine learning

INTRODUCTION

The state of key equipment for power metering, such as measuring instruments and transformers, directly affects the stable operation and measurement accuracy of the power system. Traditional monitoring methods rely on manual inspections, making it difficult to achieve real-time state monitoring of equipment, resulting in delayed information acquisition, difficulty in predicting potential failures, increased system operational risks, and low efficiency. In addition, traditional health prediction methods are limited by statistical analysis and signal processing techniques, resulting in insufficient accuracy and limited prediction reliability when faced with multi-dimensional complex data, which can easily lead to misjudgments and increase maintenance costs. The applicability of its model is also insufficient, as it relies only on a single data source and limited features, making it difficult to reflect the equipment state fully, and consumes large computing resources and time, which limits its practical application. To address the aforementioned challenges, intelligent monitoring and prediction solutions that integrate the Internet of Things (IoT) and machine learning technologies have attracted much attention. The Internet of Things technology utilizes intelligent sensor networks to achieve real-time data collection and monitoring of equipment state, ensuring real-time and accurate information [1,2]. Machine learning algorithms are adept at processing massive and complex data, mining deep patterns, and significantly improving the precision of health prediction and model generalization ability [3,4]. The combination of the two can not only promote the transformation of equipment management mode towards proactive prevention, effectively reduce the occurrence of faults, and extend equipment life, but also promote the efficient and intelligent development of power metering production.

This article aims to solve the problem of state monitoring and health prediction of key equipment in power metering, especially the current methods with poor real-time performance and low accuracy. This article utilizes IoT sensor networks to monitor equipment state in real-time, and uses machine learning algorithms to analyze data and accurately predict equipment health. Experiments have shown that the model in this article outperforms other models in terms of real-time performance, accuracy, and reliability, particularly in life prediction, fault assessment, and performance prediction. Compared to other current models, the innovation of this study lies in combining IoT technology to instantly collect and monitor data from power metering equipment, ensuring real-time and accurate information; at the same time, using machine learning to deeply explore data patterns has greatly improved prediction accuracy and model generalization ability. The contributions of this study include that: the experiment verifies the validity and feasibility of the proposed method, which provides an efficient and precise solution for power metering equipment management; it promotes the change of equipment management from

passive maintenance to active prevention, reduces the failure rate, prolongs the life of the equipment, and helps power metering to develop in the direction of more efficient and intelligent.

RELATED WORK

The state monitoring of power equipment is crucial for the stable operation of the power system. It can promptly detect signs of equipment failure and prevent major accidents. Effective monitoring can significantly improve equipment availability and reliability, reduce unexpected shutdowns, and ensure safe and continuous power supply [5,6]. To achieve a comprehensive analysis of online monitoring and data collection of power transmission and transformation equipment, Zhou et al used the responsibility area mechanism of the D5000 system platform, combined with other related applications, to design the system and software architecture of online monitoring applications, and obtained characteristic parameters of power equipment response state for equipment fault diagnosis, thus filling the technical gap of electrical equipment state monitoring and analysis system [7]. Portable thermal imaging equipment are unable to continuously track the state of power equipment, resulting in low efficiency. To address this issue, Wang et al proposed an online monitoring method for electrical equipment state based on infrared image temperature data visualization and processing. This method was applied in actual substations and its effectiveness was demonstrated [8]. Infrared thermography has become an indispensable tool for power equipment condition monitoring and fault diagnosis based on absolute and relative temperature values. Xia et al applied deep learning algorithms to achieve object detection in complex environments for automatic fault diagnosis, and proposed future suggestions for equipment state monitoring and diagnosis from the aspects of building intelligent infrared detection systems and comprehensively utilizing joint visualization diagnosis technology [9]. The assessment of the health state of power equipment is a widely concerned issue in the power system industry. Zhao and Cui proposed a real-time health state assessment method for wind turbines, which was based on cloud models and cloud transformations, combined with historical state data of data collection and monitoring control systems, to train the health assessment model. The results indicated that the model could detect changing trends, improve the reliability of wind turbines, and reduce maintenance costs [10]. Although scholars' research has improved the reliability of equipment monitoring, it still faces problems such as poor real-time performance, insufficient model generalization ability, and weak integration ability of multi-source data.

Deep learning can improve the accuracy of power metering equipment prediction by learning and analyzing large amounts of historical data, which is extremely important for the economic dispatch and resource optimization of the power system [11,12]. The risk prediction of power metering equipment failures can reduce the losses caused by faults in the national power grid. Liu et al used data preprocessing, feature selection, and gradient boosting decision trees for fault and equipment life prediction. Compared with other algorithms, this algorithm performed the best after optimization [13]. Zhang proposed a monitoring method based on image deep learning to address the shortcomings of fuzzy C-means clustering in power metering equipment fault monitoring. Simulation experiments showed that this method highly matched the actual curve in voltage and current monitoring, with precise monitoring, which helped power metering equipment to better function [14]. Although the methods proposed by the aforementioned scholars can to some extent address the shortcomings of traditional methods, there are still issues such as high computational complexity, low data processing efficiency, and models that rely too heavily on annotated data.

KEY EQUIPMENT STATE MONITORING AND HEALTH PREDICTION

Construction of State Perception Network

State perception network design

The Internet of Things technology is applied to the power metering state perception network, and multiple aspects such as the collection of operational information, information integration, and health assessment of power metering equipment are integrated and managed. The layout of sensors is based on an in-depth analysis of equipment state perception. Based on the above considerations, a state perception network for power metering equipment is designed. Its composition structure is shown in Figure 1:

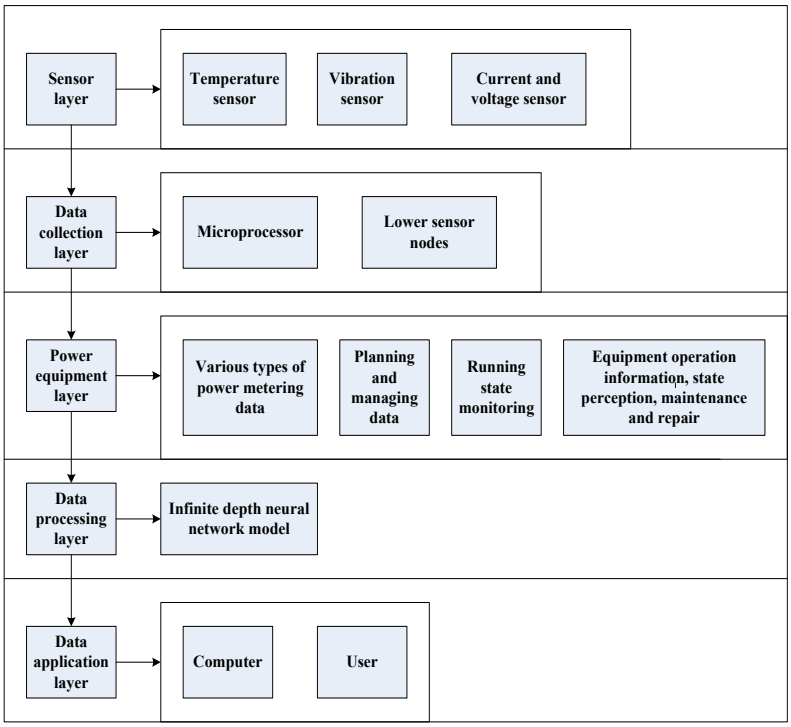

Figure 1. Composition structure of state perception network for power metering equipment

This article is based on the Internet of Things technology and uses intelligent sensors to construct a power metering equipment state perception network consisting of a sensor layer, a data acquisition layer, a power equipment layer, a data processing layer, and a data application layer, breaking through the shortcomings of traditional technology. In key parts of the power metering equipment, this article installs temperature sensors, vibration sensors, current and voltage sensors, etc., to comprehensively monitor the equipment state. The temperature sensor is located adjacent to critical electronic components, designed to capture signs of overheating and prevent measurement inaccuracies. Vibration sensors monitor mechanical components, warn abnormal vibrations, and prevent sudden failures. At the data acquisition layer, this article delegates data processing tasks to sensor nodes and equips them with microprocessors for preliminary data processing, such as filtering and anomaly detection. Sensor nodes can analyze and process signals in real-time. Once the data exceeds the safety threshold, an alarm can be triggered and abnormal data can be transmitted to the monitoring system, which improves the response speed of abnormalities and saves communication resources. At the level of power equipment, this article establishes a full lifecycle database and integrates various types of power metering data using data fusion technology. Users can extract the required information and conduct in-depth learning and training through an infinite deep neural network model, comprehensively mining the full lifecycle data of power metering assets. The data processing layer utilizes big data algorithms and deep mining algorithms to process and analyze various power data. By constructing an infinite-depth neural network model, macro data is transformed into mathematical modeling, revealing micro data more profoundly, thereby enhancing the data analysis capability of power metering assets.

Key technologies

The Internet of Things technology connects the physical world and the Internet to achieve communication and data exchange between equipment [15,16]. The Internet of Things technology integrates sensors and other equipment to sense the environment, collect data, and transmit it to the cloud for processing through wireless networks [17,18]. In power metering equipment, the Internet of Things monitors the state in real-time, collects key parameters, assists in state analysis and health prediction, and improves the stability and reliability of the power system. By using intelligent sensor networks to monitor equipment state in real-time, key parameters are collected, and machine learning models are used to analyze and process the data, which can improve prediction accuracy, achieve fault warnings, reduce maintenance costs, and extend equipment lifespan.

The power Internet of Things is a technology that integrates mobile interconnection, artificial intelligence, and digital information transmission [19,20]. In practical work, the type of power metering equipment collected by

the collection layer is *x*; the length value n_x of various data information is used as the output of power metering equipment; d is the public key parameter collected by the power metering equipment in the perception layer; h is the key value of the main key used by power metering equipment to output public key data. If $x \in \{1, \ldots, n_x\}$, then the bit value of each data bit obtained from the type of power metering equipment to be obtained is 1. At this point, the output formula for the data information obtained by the perception layer is:

$$e_x = \frac{g_j(a)(e_1, e_2)}{g'(x)} \tag{1}$$

Among them: e_x - the set value of power equipment data information obtained in the perception layer;

e_1 - the key value of the obtained data information;

e_2 - the equipment data element obtained from power equipment.

When the perception layer collects power data, the computing center organizes the data received from e_x to obtain a result. The formula is:

$$r_{e_x} = d(h_2, h_1) e_x^{h+\sum_{j=1} x_j} \tag{2}$$

Among them: r_{e_x} - the organized dataset;

h_2 and h_1 - the data to be called and the calling data;

x_j - the information on power metering equipment.

In the data calculation process, the input raw data information includes metering standard data, metering output data, appearance data information, etc.

Data Preprocessing and Feature Extraction

Data preprocessing

Due to the influence of external factors such as personnel and equipment, historical data extracted from the actual application scenarios of on-site measuring equipment often lacks data items generated by one or more domains, or contains a significant amount of information. Therefore, data preprocessing is necessary.

Data preprocessing is a key step in data mining [21,22]. The data preprocessing in this article can first reduce the amount of raw data through data sampling while preserving its features to improve subsequent processing efficiency. Then, the variable selection is used to eliminate irrelevant or missing variables, simplify data dimensions, and accelerate algorithm operation. Afterwards, missing values are processed through data replacement, and mean and median values are used to ensure data integrity. Subsequently, data noise is eliminated by filtering outliers to improve model accuracy. If certain variables are not applicable, they can be adjusted through variable substitution.

Signal denoising during operation

The data collection time for this article is from August to October, mainly at 10am. The operating parameters of the load box in power metering equipment are usually stored in the form of signals, but due to factors such as equipment vibration and environment, significant noise is generated, which seriously affects the accuracy of equipment state perception and health prediction [23]. When power metering equipment is collecting data, due to the complex background and high noise, valuable signals are often masked. This article uses the Gabor transform method to denoise it. Table 1 shows some of the collected raw data information.

In power metering equipment, the working signal of the load box is obtained by superimposing two composite harmonic signals, represented by $z(s) = e^{nv_1 s} + e^{nv_2 s}$, and the auxiliary function is represented by $\beta_{ij}(s) = (b/S)^2 e^{nvs}$. By using the Gabor transformation, it can be obtained:

$$b_{ij} = \int_{-\infty}^{+\infty} z(s)\beta_{ij}^*(s)\,dt = 2\pi(b/S)^2[\varphi(\mu - \mu_1) + \varphi(\mu - \mu_2)] \tag{3}$$

As shown in Formula (3), the Gabor expansion factor can be determined by a linear function of the frequency of

the load box signal in the equipment, and the amplitude is set to $2\pi(b/S)^2$. The use of Gabor transform can accurately extract the two frequency bands of $2\pi(b/S)^2$, fully reflecting the equipment operation state, noise characteristics and distribution, providing a basis for denoising processing of subsequent working signals.

Table 1. Basic information data of power metering equipment

Serial number	Time stamp	Equipment number	Voltage value (V)	Current value (A)	Noise level (dB)
1	2023-08-1 10:00	001	220.1	0.98	25.3
2	2023-08-5 10:00	001	220.5	0.99	25.8
3	2023-08-10 10:00	001	220.3	1.02	26.1
4	2023-08-15 10:00	001	219.9	1.01	25.9
5	2023-08-20 10:00	001	220.2	0.97	26.2
6	2023-08-25 10:00	001	220.4	1.03	25.7
7	2023-08-30 10:00	001	220.6	1.04	25.6
8	2023-09-1 10:00	001	220.0	0.96	26.3
9	2023-09-5 10:00	001	220.5	1.05	25.5
10	2023-09-10 10:00	001	220.2	1.00	26.0
11	2023-09-15 10:00	001	220.3	1.01	25.8
12	2023-09-20 10:00	001	220.4	0.99	26.1
13	2023-09-25 10:00	001	220.1	1.02	25.7
14	2023-10-1 10:00	001	220.6	1.03	25.9
15	2023-10-5 10:00	001	220.5	0.98	26.2

Based on the above analysis, an appropriate threshold y is selected to further process the results of Formula (3). The formula is:

$$b'_{ij} = \begin{cases} b_{ij} & |b_{ij}| > y \\ 0 & |b_{ij}| \le y \end{cases} \tag{4}$$

Among them: b'_{ij} - the higher Gabor expansion coefficient of the signal energy of the equipment in a working state;

b_{ij} - the Gabor expansion coefficient at runtime.

According to the result of Formula (4), a set of noise-reduced equipment operation signals is reconstructed and obtained, which are expressed as follows:

$$z'(g) = \sum_{i=0}^{I-1} \sum_{j=0}^{M-1} b'_{ij} k(l - iS) e^{nj\Omega l} \tag{5}$$

Generally speaking, the reconstructed result $z'(g)$ of Formula (5) has a higher signal-to-noise ratio than the original signal $z(g)$. This indicates that by selecting an appropriate threshold, the Gabor transform can effectively suppress noise [24,25]. Then, using sampling rate and Gabor transform to perform correlation analysis on the threshold, the optimal threshold y is obtained.

When using the Gabor transform for noise suppression, the relationship between various parameters can be expressed as:

$$s_b = \sqrt{\frac{2}{\tau I}} \delta_M \cdot inverf(q) \tag{6}$$

Among them: τ - the sampling rate;

I - the sample size;

δ_M - the noise standard deviation;

$inverf(q)$ - the inverse of the error function.

When q=0.99, the denoising effect of the Gabor transform is optimal, and the threshold y is set to s_b. Therefore, the expression of the threshold y is as follows:

$$y = \sqrt{\frac{2}{\tau I}}\delta_M \cdot \text{inverf}(0.99) = 2.5758 \cdot \frac{\delta_M}{\sqrt{\tau I}} \quad (7)$$

According to Formula (7), the optimal threshold is obtained, and Formula (5) is used to denoise the operating signal to obtain the best denoising effect, laying the foundation for subsequent evaluation of the operating state. The original noise reduction effect and the Gabor transformed running signal noise reduction effect are shown in Figure 2:

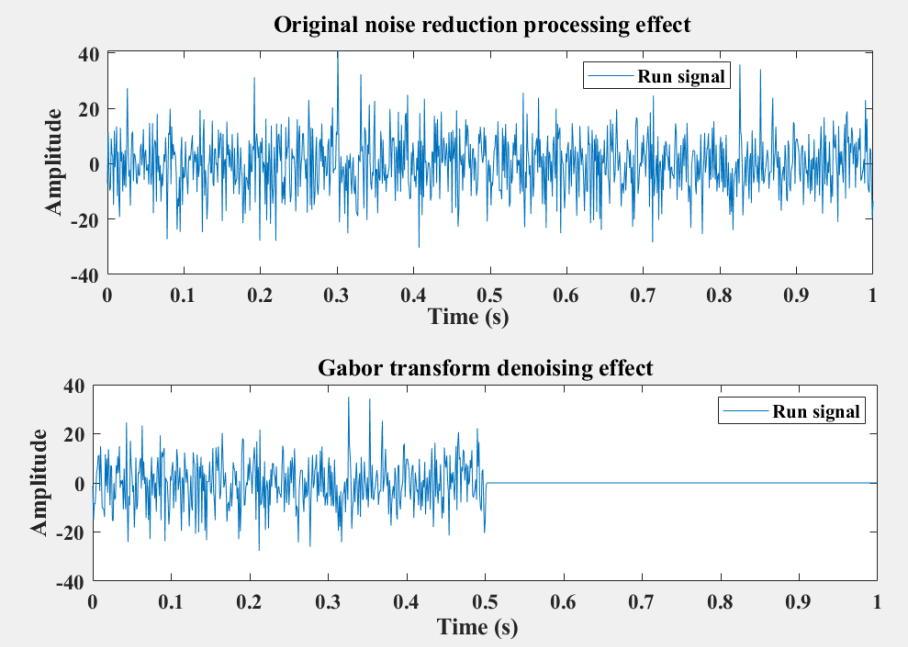

Figure 2. Comparison of noise reduction effects

The upper graph of Figure 2 shows the signal variation within 1 second. Due to the addition of significant random noise, the signal is mixed with high amplitude random fluctuations, masking the original sine waveform and making it difficult to identify the true characteristics of the signal. The below graph in Figure 2 shows the signal processed by the Gabor filter. It can be seen that the filtered signal to some extent suppresses random noise, making the overall waveform of the signal smoother and the original sine wave shape clearer. In summary, the Gabor transform has successfully reduced the impact of noise, enhanced the main frequency components of the signal, and made the characteristics of the original signal more prominent, making it suitable for subsequent signal analysis or fault diagnosis applications.

Evaluation of equipment operation state

After completing the noise reduction of the operating signal of the power equipment load box, the working condition of the equipment after noise suppression is analyzed to extract the state characteristic signals of the equipment, and the working condition evaluation criteria are set to evaluate its working condition. The operating state characteristic signals of the power equipment load box include two types of characteristic signals: operation and stability.

The reference values for evaluating the operating state of power equipment load boxes can be set as follows:

$$\overline{B} = \frac{(b_1 + b_2 + \cdots + b_i)}{i} \quad (8)$$

Among them: $\overline{B}$ - using the average characteristic signal of the operating state of power metering equipment as the evaluation benchmark.

i - the number of characteristic signals.

Then, the operational state evaluation warning range of the equipment is:

$$\begin{cases} B_d = \overline{B} \pm 3\vartheta \\ \vartheta = \sqrt{\frac{1}{i-1}\sum_{n=1}^{i}(B_n - \overline{B})^2} \end{cases} \quad (9)$$

Among them: B_d - the warning range for operational state assessment;

ϑ - the standard deviation;

B_n - the evaluation benchmark value for the nth feature signal.

Based on the basic measuring points of power metering equipment, the warning interval for evaluating the working condition of the equipment is calculated using the above formula, as shown in Table 2.

Table 2. Warning interval table for equipment operation state perception

Serial number	Name of measuring point	Standard deviation	Warning interval
1	Upper guide swing	5.1	100.3-150.00
2	Lower guide deflection	6.8	138.02-172.49
3	Hydraulic deflection	9.16	90.42-139.15
4	Horizontal vibration of upper frame	0.41	1.79-8.36
5	Horizontal vibration of lower rack	2.63	12.54-19.68
6	Vertical vibration of upper frame	1.50	12.00-18.00
7	Vertical vibration of lower rack	2.20	24.00-30.00
8	Spindle runout	3.10	62.10-77.90
9	Rotor runout	4.50	90.00-120.00
10	Stator temperature	10.00	80.00-120.00

According to the warning interval in Table 2, it is possible to conduct an in-depth analysis of the operational state of power metering key equipment. If the operating signal value of the equipment is within the warning range, it indicates an abnormal state, and further diagnosis is required. Table 2 contains 10 measuring points, their standard deviations, and warning ranges. The standard deviation of the upper guide deflection is 5.1, and the warning range is 100.3-150.00, which means that its value may be abnormal if it exceeds this range. For vibration measuring points, if the horizontal vibration of the upper frame has a small standard deviation and a narrow warning range, it indicates that the vibration is relatively stable. For the stator temperature, the standard deviation is 10.00 and the warning range is 80.00-120.00, indicating significant temperature fluctuations and the need for strict temperature control to prevent overheating. By monitoring these measuring points in real-time and comparing them with the warning interval, the equipment state can be effectively monitored; problems can be detected and dealt with promptly; the safe and stable operation of the equipment can be ensured.

Feature signal extraction

By collecting historical information on power equipment load boxes and using empirical mode decomposition algorithm to identify them, a basis is provided for constructing predictive models in the future. The empirical mode decomposition algorithm essentially decomposes the signal changes or trends at different scales by smoothing the signal, extracts a series of feature signals at different scales, and uses them as a set of IMF (Intrinsic Mode Function) components [26,27].

The first step in extracting the operating characteristic signals of power metering equipment is to precisely locate the local extreme points in the historical operating data x(t) of the equipment. Subsequently, to deeply analyze the operating state of the equipment, an efficient cubic spline interpolation technique is used to construct the upper and lower envelope lines of the signal. By mathematically processing these two envelope lines, their local means are calculated using the formula:

$$w(s) = \frac{v_1(s)+v_2(s)}{2} \quad (10)$$

Among them, $v_1(s)$ and $v_2(s)$ respectively refer to the numerical values of the upper and lower envelopes.

Then, making $f(s) = a(s) - w(s)$, and if $f(s)$ cannot meet the IMF's standards, it is determined as the new $a(s)$. The second step can be repeated to obtain:

$$f_{1l}(s) = f_{1(l-1)}(s) - w_{1l}(s) \tag{11}$$

In practical applications, due to multiple iterations, the amplitude of the IMF component tends to be constant, thus losing its practical significance. Therefore, this article adopts the standard deviation Z_D iteration termination condition to ensure the practical significance of the IMF component, and the formula is:

$$Z_D = \sum_{s=0}^{S} \left[\frac{f_{1(l-1)}(s) - f_{1l}(s)}{f_{1(l-1)}(s)}\right]^2 \tag{12}$$

Afterwards, the first IMF component of the operating signal of the power metering equipment and its residual terms are calculated, and the formula is:

$$\begin{cases} E_1 = f_{1l}(s) \\ t_1(s) = a(s) - E_1 \end{cases} \tag{13}$$

Among them: E_1 - the first IMF component of the operation signal of the power metering equipment;

$t_1(s)$ - the remaining terms of the operating signal.

Finally, the residual part of the operating signal is filtered to obtain all IMF components of the operating signal until $t_n(s)$ approaches zero infinitely. At this point, the characteristic signal E_n of the power metering equipment operation is obtained.

Construction of Health Prediction Model

Health prediction is a prediction method based on statistical principles and mathematical models. It fully utilizes the past or present information of the target being predicted, and constructs a prediction model using machine learning and other methods to predict the trend and possible values of the target. In the in-depth study of power metering equipment data, it is found that the temporal characteristics, nonlinear characteristics, and small sample situations make it difficult for a single model to make precise predictions. Therefore, this article studies a combination prediction method that obtains more accurate prediction results by calculating the weighting coefficients of each model. Traditional trial and error methods and expert weighting methods are prone to local extremum when determining weight coefficients, and global search methods must be used. To address this issue, in order to avoid getting stuck in local optima when searching for the optimal solution, this article adopts an improved grey wolf optimizer algorithm to search for the optimal weight coefficients, thereby improving search efficiency and global optimization capability. At the same time, to solve the problem of poor prediction effect of a single model when dealing with complex data, a combined prediction model is established to improve the accuracy and reliability of its prediction (for aging of measuring instrument elements).

Grey Wolf Optimizer (GWO) is a new intelligent optimization algorithm that has emerged in recent years. It simulates the hunting behavior of wolf packs and obtains the optimal solution through communication and self-regulation among different levels of grey wolves. GWO has strong global optimization ability, universality, and robustness [28,29]. In the grey wolf optimizer algorithm, the selection, exploration, and tracking behaviors of grey wolves are adjusted to achieve global search and optimization. When solving complex problems, traditional linear iterative methods are often constrained and cannot accurately reflect the real environment, resulting in inaccurate results and even reduced algorithm execution efficiency. To address this issue, it is necessary to improve and optimize c using the following nonlinear convergence factor expression:

$$c' = 2(c_{ini} - c_{end}) \cdot \left(1 + e^{1-\frac{q}{Q_{Max}}}\right) \tag{14}$$

Among them: c_{ini} - modifying the starting value of the nonlinear factor c';

c_{end} - the termination value;

Q_{Max} - the maximum number of iterations;

q - the current iteration count.

The comparison between the traditional convergence factor and the improved nonlinear convergence factor is shown in Figure 3:

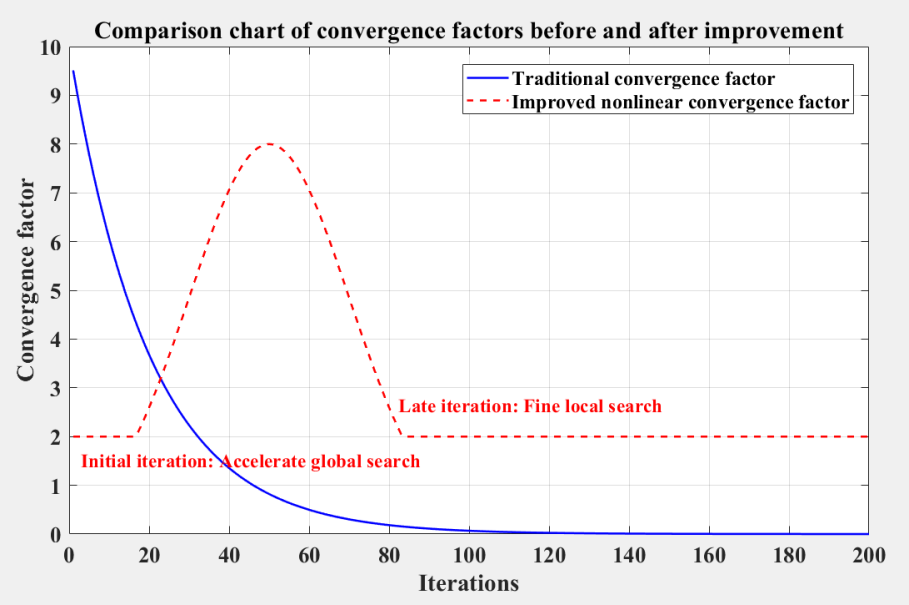

Figure 3. Comparison of convergence factors

Figure 3 compares the convergence factors of traditional and improved methods. The horizontal axis represents the number of iterations, and the vertical axis represents the size of the convergence factor. The traditional convergence factor decays exponentially with the number of iterations, and the decay rate is fast, decreasing from 9.5 to 0, indicating that the algorithm gradually reduces the search range and tends to converge. The improved nonlinear convergence factor adopts a Gaussian function, which first stabilizes, then increases, and gradually decreases and tends to stabilize after reaching the highest value. This makes the algorithm emphasize global search in the early stage, quickly exploring the solution space, and later focusing on local search, finely adjusting the solution. The comparison shows that the improved design is more reasonable and can improve the global search and local convergence accuracy of the algorithm. The traditional convergence factor has limitations in both global and local search, and cannot be fully optimized due to limitations. The improved nonlinear convergence factor can enhance the performance of the wolf pack algorithm, accelerating global search in the initial stage and enabling more refined local search in the later stage, thereby improving the algorithm's local search capability.

Machine learning is an important research direction in the field of health prediction for power metering equipment. Among them, the autoregressive moving average method, radial basis function neural network, and least squares support vector machine have shown good performance in this area and have been verified in practice. To further improve its accuracy, a joint prediction model is constructed based on the above single prediction model to enhance the accuracy of the prediction. On this basis, combined with the characteristics of differential changes and periodic patterns in time series, as well as nonlinear characteristics and small sample situations, an improved grey wolf optimizer algorithm is used to search for the optimal weight coefficients and establish a combination prediction model. The prediction results are obtained by the weighted sum of the predicted values of each single model.

To maximize the advantages of the combination prediction model, based on optimization theory, this article selects the root mean square error function as the fitness function of the improved grey wolf optimizer algorithm, thereby transforming the search for the optimal weight coefficients into an optimization problem of minimizing the root mean square error. The formula is:

$$\mathrm{RMSE}_{\min} = \sqrt{\frac{1}{\mathrm{m}}\sum_{\mathrm{j}=1}^{\mathrm{m}}\left(\mathrm{r_j} - \tilde{\mathrm{r}}_{\mathrm{j}}\right)^2} \tag{15}$$

Among them: r_j - the true value;

$\tilde{r}_j$ - the predicted value.

The prediction process of the health prediction model based on the improved grey wolf optimizer algorithm is as

follows. The size of the wolf pack is initialized, including the number of members, spatial position of the wolves, convergence factor, disturbance factor, and maximum number of iterations. Three models are used: autoregressive moving average, radial basis function neural network, and least squares support vector machine for prediction, and parameters are adjusted to achieve optimal results. The wolf pack is substituted into the combination model, and the top three positions are determined by comparing their fitness values and assigned to the corresponding wolves. At the same time, the position vector of the optimization target is also assigned corresponding values. According to Formula (14), the values of the convergence factor and perturbation factor are calculated. After the next iteration, the positions of each wolf and the optimal solution are calculated. Whether the improved grey wolf optimizer algorithm reaches the maximum number of iterations is judged. If achieved, the optimal solution position information is utilized to calculate the output optimal weight coefficients; otherwise, it is proceeded to the third step. When the grey wolf optimizer algorithm reaches its maximum number of iterations, the iteration is stopped. The optimal weight coefficient obtained is multiplied by each single model to obtain the combination prediction result. This process improves the accuracy and efficiency of health prediction by optimizing the weight coefficients of the combination model through the grey wolf optimizer algorithm.

DEMONSTRATION ON STATE PERCEPTION AND HEALTH PREDICTION OF POWER METERING EQUIPMENT

Experimental Design and Data Sources

The purpose of this experiment is to verify the effectiveness and feasibility of combining IoT and machine learning for state perception and health prediction. This method mainly monitors the state of power metering equipment in real-time through the Internet of Things sensor network, and uses machine learning algorithms to analyze data to predict the health of the equipment. The experiment utilizes various detection methods and advanced algorithms to comprehensively evaluate the equipment. The data is sourced from real-time operational data of power metering equipment, including basic information, voltage, current, and noise, collected from August 1st to October 5th, 2023. After collecting data, it is cleaned, preprocessed, and standardized to eliminate invalid data and unify indicator units for subsequent analysis. Finally, the prediction results are analyzed by comparing the real-time performance, prediction accuracy, and reliability of the hybrid expert model based on federated learning, the smart meter measurement error prediction framework, the smart meter prognostics and health management model, and the combination prediction model of the improved grey wolf optimizer algorithm proposed in this article. Considering that the performance parameters of power metering equipment also affect the experimental results and conclusions, it is necessary to determine and display them before the experiment, as shown in Table 3:

Table 3. Performance parameters related to power metering equipment

Serial number	Classification	Performance parameter	Numerical settings
1	Input measurement	Rated power factor	>0.9
2		Instantaneous overload capacity	1.5 times the rated current
3		Working frequency range	45 Hz - 65 Hz
4	Safety protection	Protection level	IP54
5		Anti electromagnetic interference capability	EN 61000-6-3
6	Power waste	Average power consumption	<0.5 VA
7		Standby power	<0.1 VA
8		Activate power consumption	<1 VA
9	Other characteristics	Temperature working range	-20℃ - +60℃
10		Humidity working range	10%RH - 90%RH
11		Storage temperature range	-40℃ - +85℃
12		Storage humidity range	5%RH - 95%RH

The Hybrid Expert Model Based on Federated Learning (HEM-FL) is designed to analyze and identify alarm information in power metering systems. Through federated learning partitioning problems, it improves recognition and prediction accuracy and is suitable for distributed environments that value data privacy. The Smart Meter Measurement Error Prediction Framework (SM-MEPF) focuses on predicting meter measurement errors, which is crucial for ensuring accurate power metering and monitoring equipment health, especially for smart grids that rely on precise data. The Smart Meter Prognostics and Health Management Model (SM-PHM) combines fault

identification and health management to predict potential faults through real-time data, improving equipment reliability and lifespan.

Experimental Results

Real-time performance

Real-time performance is a key indicator for evaluating model performance, which can measure the rapid response of health prediction models to equipment data and ensure timely warning in case of abnormalities. The system's response speed is evaluated through data processing time to meet real-time monitoring and rapid decision-making requirements, and enhance equipment safety and stability. Therefore, this article conducts 15 tests on the collection and processing time of equipment state data, and tests the data collection and processing time of each method to evaluate the response speed of its model. The results are shown in Figure 4:

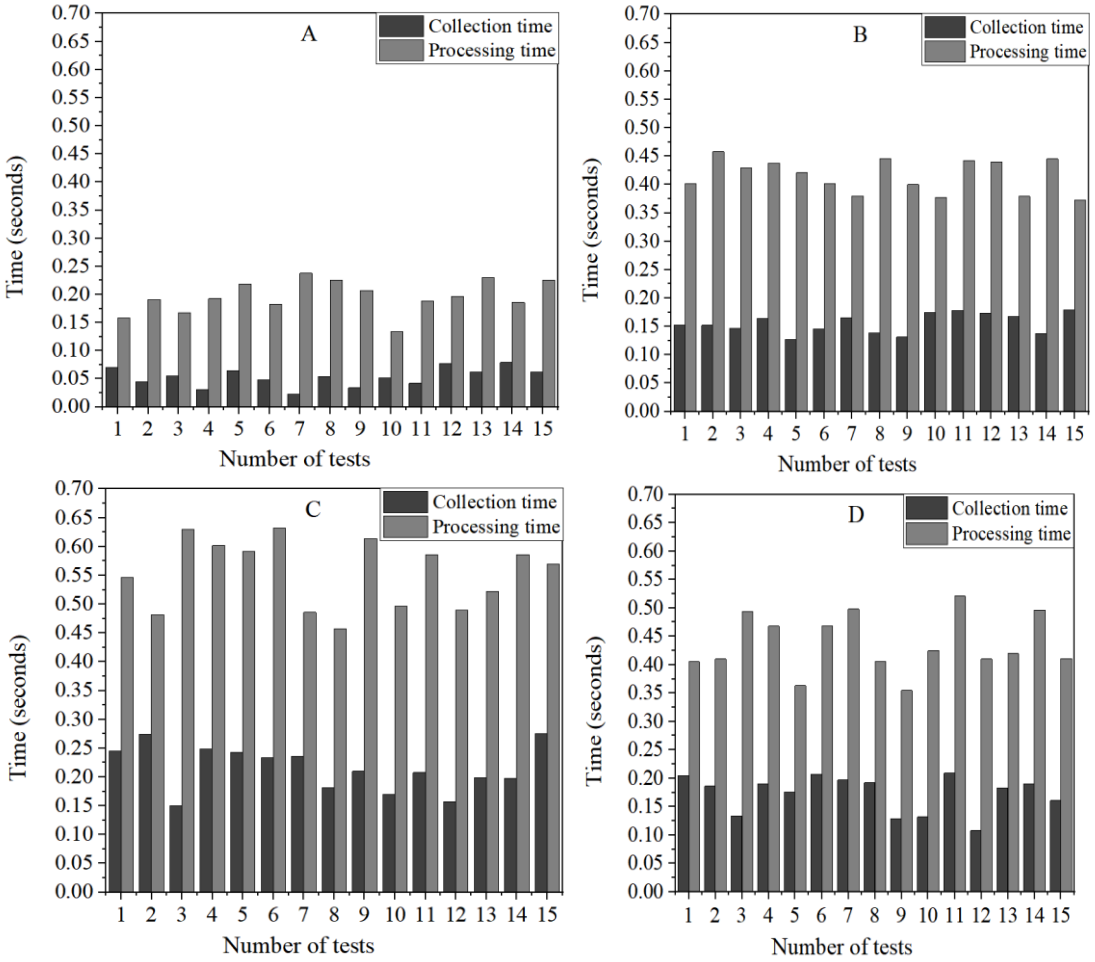

Figure 4. Equipment collection and processing time under different models. (A): Collection and processing time under the model presented in this article; (B): Collection and processing time under the HEM-FL model; (C): Collection and processing time under the SM-MEPF model; (D): Collection and processing time under the SM-PHM model.

According to Figures 4 (A), 4 (B), 4 (C), and 4 (D), it can be seen that for the model in this article, the data collection time ranges from 0.023 seconds to 0.079 seconds in 15 tests, with an average of about 0.053 seconds, while the data processing time ranges from 0.134 seconds to 0.238 seconds, with an average of about 0.196 seconds. Compared to other models, this model demonstrates significant advantages in data collection and processing time. The HEM-FL model has an average collection time of 0.155 seconds and an average processing time of 0.415 seconds; the SM-MEPF model has an average collection time of 0.215 seconds and an average processing time of 0.553 seconds; the SM-PHM model has an average collection time of 0.173 seconds and an average processing time of 0.437 seconds. The model in this article can complete data collection and processing

more quickly, thus responding to changes in the state of power metering equipment in a timely manner, which is crucial for improving the safety and stability of the power system. This advantage makes the model in this article have a wide range of application prospects in the power industry.

Prediction accuracy

Prediction accuracy is the key to accurately assessing the equipment state of the evaluation model. Quantifying the prediction effect through indicators such as accuracy ensures that the model precisely identifies the health state and faults of equipment, improves management efficiency, and reduces maintenance costs. Therefore, this article uses evaluation indicators such as accuracy, precision, and recall to quantify the performance of the health prediction model, and calculates the accuracy, precision, and recall of the model in 15 tests. The results are shown in Figure 5:

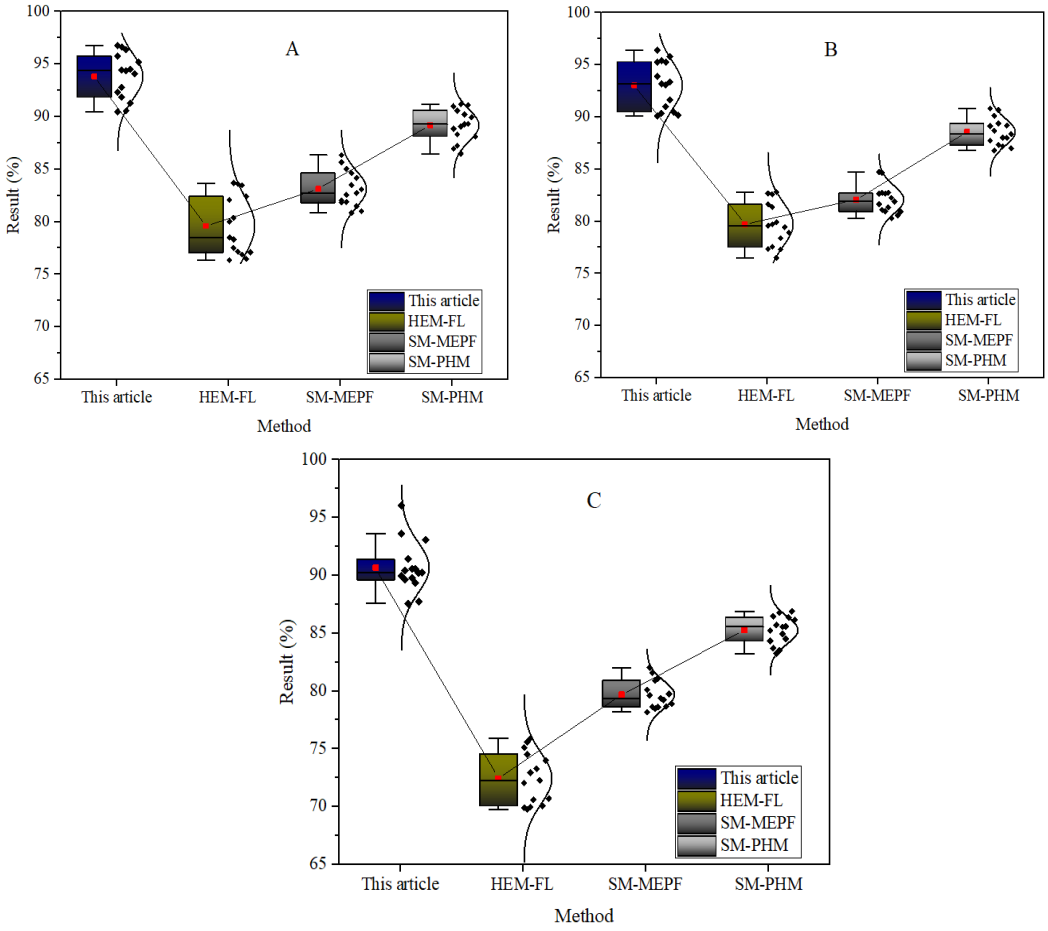

Figure 5. Comparison of accuracy, precision, and recall results of the model (A): Comparison of accuracy results of four models; (B): Comparison of precision results of four models; (C): Comparison of recall results for four models;

As shown in Figure 5 (A), the model in this article performs well in most cases. In the 9th test, the accuracy of the model reaches 96.84%, far exceeding the 83.60% of the HEM-FL model, 80.83% of the SM-MEPF model, and 89.10% of the SM-PHM model. Overall, the average accuracy of the model in this article reaches 93.84%, demonstrating its effectiveness in determining the health state of power metering equipment. Figure 5 (B) shows that the model in this article also performs well in terms of precision. Taking the first test as an example, the precision of the model in this article is 96.48%, while the precision of HEM-FL model, SM-MEPF model, and SM-PHM model are 81.65%, 82.63%, and 87.74%, respectively, which are significantly higher than other models. This indicates that it can not only accurately predict equipment state, but also effectively reduce false alarms and ensure the reliability of prediction results. The recall data in Figure 5 (C) further demonstrates the advantages of the model in this article. In the second test, the recall rate of the model in this article is 96.08%, far higher than

the 74.58% of the HEM-FL model, 79.64% of the SM-MEPF model, and 84.33% of the SM-PHM model. This means that the model can more comprehensively identify actual fault situations and reduce false negatives. This indicates that the accuracy, precision, and recall of the model in this article are good, confirming its high accuracy and reliability in power metering equipment state perception and health prediction. This model can help power companies find potential equipment problems in advance, optimize maintenance strategies, reduce costs and improve equipment management efficiency.

Reliability

In power metering, the fault warning rate and false alarm rate of the model are important indicators for measuring the reliability and stability of the prediction model. They reflect the accuracy of the model's fault prediction and its ability to avoid false alarms. Reliability testing is crucial for equipment state perception and health prediction, ensuring accurate predictions and system stability, reducing resource waste caused by false alarms, and improving efficiency. Therefore, this article tests the fault warning rate and false alarm rate of four models. The results are shown in Figure 6:

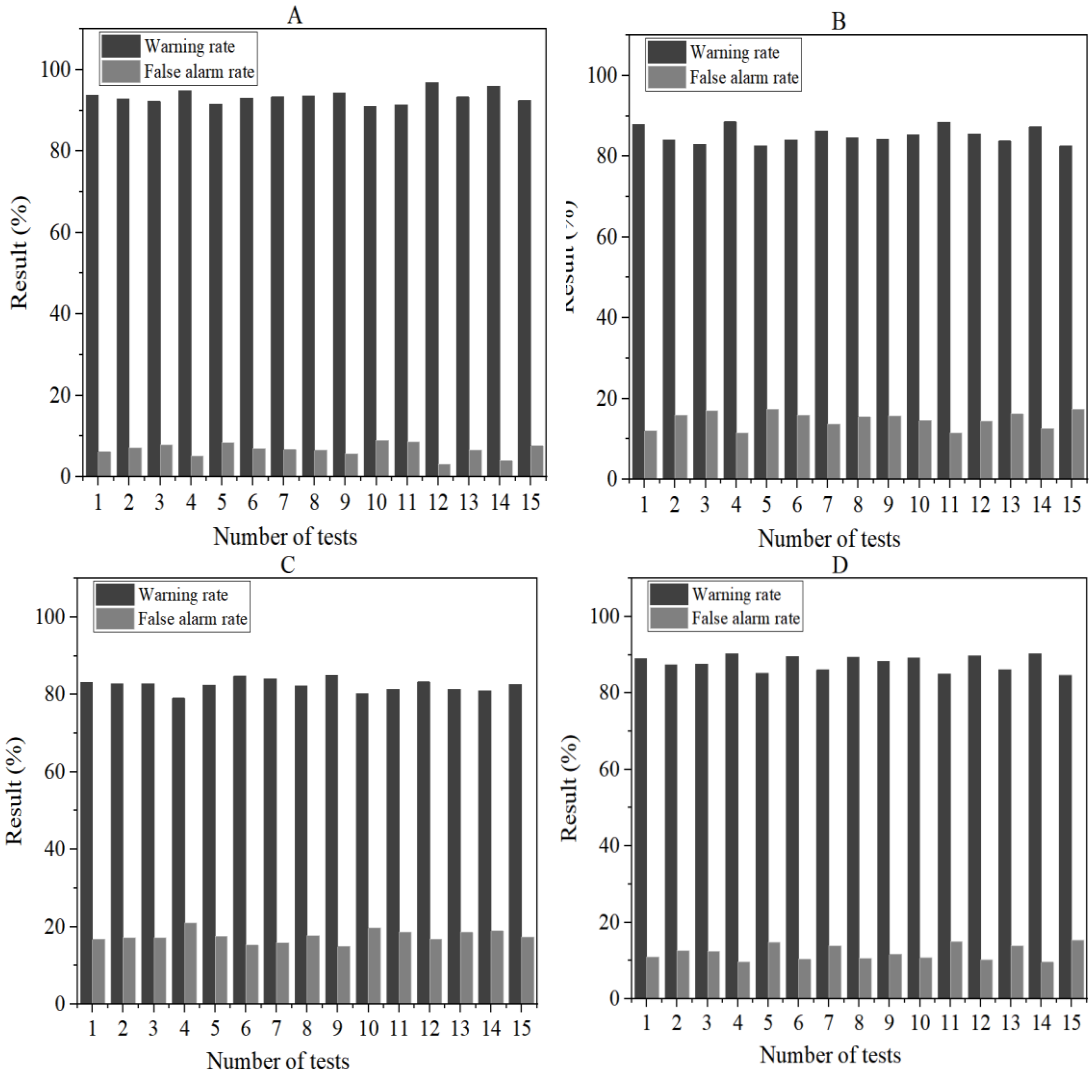

Figure 6. Comparison of fault warning rate and false alarm rate among four models (A): Fault warning rate and false alarm rate under the model presented in this article; (B): Fault warning rate and false alarm rate under the HEM-FL model; (C): Fault warning rate and false alarm rate under the SM-MEPF model; (D): Fault warning rate and false alarm rate under the SM-PHM model.

As shown in Figure 6 (A), Figure 6 (B), Figure 6 (C), and Figure 6 (D), the model in this article performs outstandingly in most of the 15 test samples. In the first test, the fault warning rate reaches 93.85%, with a false

alarm rate of only 6.15%. In the 12th sample, it is as high as 96.94%, with a false alarm rate of only 3.06%. The average fault warning rate is 93.37%, with a false alarm rate of 6.63%. In contrast, the HEM-FL model has a lower fault warning rate, ranging from 82.58% to 88.55%, and a false alarm rate of 11.45% to 17.42%; the fault warning rate of the SM-MEPF model is generally lower, ranging from 79.05% to 85.05%, with a false alarm rate of 14.95% to 20.95%; the fault warning rate of the SM-PHM model remains at a high level, ranging from 84.64% to 90.37%, with a false alarm rate of 9.63% to 15.36%. In summary, the model presented in this article not only has a high fault warning rate, but also a low false alarm rate. This indicates that the model can accurately warn of faults while effectively reducing unnecessary alarms. Therefore, it has shown good reliability and stability in the state perception and health prediction of power metering equipment.

From the above comparative experiments, it can be seen that the model proposed in this article has better real-time performance, prediction accuracy, and reliability, and its application effect is better. Therefore, this article extracts data from different time periods from three perspectives: remaining life, fault risk rate, and performance change trend, and uses this model to predict the health of power metering equipment. The predicted values are shown in Table 4:

Table 4. Model predicted results values

Prediction time	Remaining life (days)	Fault risk rate	Performance change trend (%)
2023-08-1	300	0.05	-0.2
2023-08-5	295	0.06	-0.3
2023-08-10	290	0.07	-0.4
2023-08-15	285	0.08	-0.5
2023-08-20	280	0.09	-0.6
2023-08-25	275	0.10	-0.7
2023-08-30	270	0.11	-0.8
2023-09-1	265	0.12	-0.9
2023-09-5	260	0.13	-1.0
2023-09-10	255	0.14	-1.1
2023-09-15	250	0.15	-1.2
2023-09-20	245	0.16	-1.3
2023-09-25	240	0.17	-1.4
2023-10-1	235	0.18	-1.5
2023-10-5	230	0.19	-1.6

According to the data in Table 4, it can be seen that the model proposed in this article performs well in the state perception and health prediction of key equipment in power metering production. During the time span from August 1, 2023 to October 5, 2023, this model conducts 15 health predictions on the equipment, and the results show that the remaining life of the equipment gradually decreases over time, from the initial 300 days to the final 230 days. At the same time, the failure risk rate also increases, gradually rising from the initial 0.05 to 0.19, indicating that the likelihood of equipment faults is gradually increasing. In addition, the performance trend of the equipment shows a negative value and the value gradually increases, from -0.2% to -1.6%, indicating that the performance of the equipment is gradually declining. These data strongly demonstrate the effectiveness of the model in this article in predicting the health of power metering equipment. It can not only help plan equipment maintenance and replacement in advance, but also ensure the stable operation of the power system, and reduce unexpected downtime and maintenance costs caused by equipment faults.

CONCLUSIONS

This study innovatively combined IoT and machine learning technologies to propose a state perception and health prediction method for key equipment in power metering production. Through the Internet of Things sensor network, real-time monitoring of equipment state was achieved, and advanced machine learning algorithms were used to analyze and model the collected data, thereby precisely predicting the health state of equipment. Experimental results showed that compared to other models, the model in this article exhibited significant advantages in real-time performance, prediction accuracy, and reliability, especially in residual life, fault risk assessment, and performance change prediction. In addition, compared with other models, this model also performed well. This not only helps power companies to plan equipment maintenance and replacement in advance,

ensuring stable operation of the power system, but also effectively reduces downtime and maintenance costs caused by equipment faults. However, there are still shortcomings in the research, such as the model's generalization ability, multi-source data integration ability, and data processing efficiency, which need to be further strengthened. In the future, efforts need to be made to improve the generalization ability of models, develop more efficient data integration algorithms, and explore ways to reduce dependence on annotated data, in order to further enhance the efficiency and accuracy of predictions.

ACKNOWLEDGMENT

This work was supported by State Grid Guide Project: Research on the Adaptability Analysis, Defense, and Evaluation Technology of Complex Electromagnetic Fields for Intelligent Energy Meters Project Number: 5700-202313267A-1-1-Z

REFERENCES

[1] SW Nourildean, MD Hassib, YA Mohammed, "Internet of things based wireless sensor network: a review," Indones. J. Electr. Eng. Comput. Sci, vol.27, no.1, Sept.2022, pp.246-261. DOI:10.11591/ ijeecs. v27. i1. pp246-261

[2] LL Hung, "Intelligent sensing for internet of things systems. Journal of Internet Technology," vol.23, no.1, Sept.2022, pp.185-191.

[3] I Shcherbatov, E Lisin, A Rogalev, G Tsurikov, M Dvořák, W Strielkowski, "Power equipment defects prediction based on the joint solution of classification and regression problems using machine learning methods," Electronics, vol.10, no.24, Sept.2021, pp.3145. https://doi.org/10.3390/electronics10243145

[4] C Yang, B Gunay, Z Shi, W Shen, "Machine learning-based prognostics for central heating and cooling plant equipment health monitoring," IEEE Transactions on Automation Science and Engineering, vol.18, no.1, Sept.2020, pp.346-355.DOI: 10.1109/TASE.2020.2998586

[5] EK Ukiwe, SA Adeshina, J Tsado, "Techniques of infrared thermography for condition monitoring of electrical power equipment," Journal of Electrical Systems and Information Technology, vol.10, no.1, Sept.2023, pp.49.https://doi.org/10.1186/s43067-023-00115-z

[6] J Chen, J Jiang, B Zhu, "Iot-based power detection equipment management and control system," Journal of Intelligent Systems, vol.31, no.1, Sept.2022, pp.1229-1245. https://doi.org/10.1515/jisys-2022-0127

[7] GP Zhou, HH Luo, WC Ge, YL Ma, S Qiu, LN Fu, "Design and application of condition monitoring for power transmission and transformation equipment based on smart grid dispatching control system," The Journal of Engineering, vol.2019, no.16, Sept.2019, pp.2817-2821. https://doi.org/10.1049/joe.2018.8456

[8] J Wang, J Ou, Y Fan, L Cai, M Zhou, "Online monitoring of electrical equipment condition based on infrared image temperature data visualization," IEEJ Transactions on Electrical and Electronic Engineering, vol.17, no.4, Sept.2022, pp.583-591. https://doi.org/10.1002/tee.23545

[9] C Xia, M Ren, B Wang, M Dong, G Xu, J Xie, J., et al, "Infrared thermography-based diagnostics on power equipment: State-of-the-art," High Voltage, vol.6, no.3, Sept.2021, pp.387-407. https://doi.org/10.1049/hve2.12023

[10] W Zhao, M Cui, "Real-time health status evaluation for electric power equipment based on cloud model," International Journal of Simulation and Process Modelling, vol.15, no.1-2, Sept.2020, pp. 134-144.https://doi.org/10.1504/IJSPM.2020.106974

[11] FM Dahunsi, OR Olakunle, AO Melodi, "Evolution of electricity metering technologies in Nigeria," Nigerian Journal of Technological Development, vol.18, no.2, Sept.2021, pp. 152-165. DOI:10.4314/ njtd. v18i2.10

[12] M Liu, D Liu, G Sun, Y Zhao, D Wang, F Liu, et al, "Deep learning detection of inaccurate smart electricity meters: A case study," IEEE Industrial Electronics Magazine, vol.14, no.4, Sept.2020, pp. 79-90.DOI: 10.1109/MIE.2020.3026197

[13] LIU Jinshuo, LIU Biwei, Z Mi, L Qin, "Fault Prediction of Power Metering Equipment Based on GBDT [J]," Computer Science, vol.46, no. S1, Sept.2019, pp. 392-396.

[14] HY Zhang, "Electric power metering equipment fault monitoring method based on image deep learning," Electronic Design Engineering, vol.29, no.9, Sept.2021, pp.103-106. DOI:10.14022/j. issn1674-6236.2021.09.022

[15] S Villamil, C Hernández, G Tarazona, "An overview of internet of things," Telkomnika (Telecommunication Computing Electronics and Control, vol.18, no.5, Sept.2020, pp.2320-2327.DOI: http://doi.org/10.12928/telkomnika.v18i5.15911

[16] A Bouguettaya, QZ Sheng, B Benatallah, AG Neiat, S Mistry, A Ghose, "An internet of things service roadmap," Communications of the ACM, vol.64, no.9, Sept.2021, pp.86-95.

[17] H Landaluce, L Arjona, A Perallos, F Falcone, I Angulo, F Muralter, "A review of IoT sensing applications and challenges using RFID and wireless sensor networks," Sensors, vol.20, no.9, Sept.2020, pp.2495.https://doi.org/10.3390/s20092495

[18] F Song, M Zhu, Y Zhou, I You, H Zhang, "Smart collaborative tracking for ubiquitous power IoT in edge-cloud interplay domain," IEEE Internet of Things Journal, vol.7, no.7, Sept.2019, pp.6046-6055.DOI: 10.1109/JIOT.2019.2958097

[19] H Liao, Z Jia, Z Zhou, Y Wang, H Zhang, S Mumtaz, "Cloud-edge-end collaboration in air–ground integrated power IoT: A semidistributed learning approach," IEEE Transactions on Industrial Informatics, vol.18, no.11, Sept.2022, pp.8047-8057.DOI: 10.1109/TII.2022.3164395

[20] T Ahmad, MN Aziz, "Data preprocessing and feature selection for machine learning intrusion detection systems," ICIC Express Lett, vol.13, no.2, Sept.2019, pp.93-101. DOI:10.24507/icicel.13.02.93

[21] A Zhu, Z Xiao, Q Zhao, "Power data preprocessing method of mountain wind farm based on POT-DBSCAN," Energy Engineering, vol.118, no.3, Sept.2021, pp.549-563. https://doi.org/10.32604/EE.2021.014177

[22] SB Taieb, JW Taylor, RJ Hyndman, "Hierarchical probabilistic forecasting of electricity demand with smart meter data," Journal of the American Statistical Association, vol.116, no.533, Sept.2021, pp.27-43. https: //doi.org/10.1080/01621459.2020.1736081

[23] S Das, S Khatri, A Saha, "Position sensitive detector based non-contact vibration measurement with laser triangulation method utilizing Gabor Transform for noise reduction," Journal of Vibration and Control, vol.30, no.9-10, Sept.2024, pp.1984-1994. https://doi.org/10.1177/10775463231173842

[24] Z.X Dai, "Fault diagnosis technology for power metering equipment operation based on Gabor transformation," Public Electricity Consumption, vol.39, no.04, Sept.2024, pp.42-43.

[25] N Bokde, A Feijóo, D Villanueva, K Kulat, "A review on hybrid empirical mode decomposition models for wind speed and wind power prediction," Energies, vol.12, no.2, Sept.2019, pp.254.https://doi.org/10.3390/en12020254

[26] Z Zhang, WC Hong, "Electric load forecasting by complete ensemble empirical mode decomposition adaptive noise and support vector regression with quantum-based dragonfly algorithm," Nonlinear dynamics, vol.98, no.2, Sept.2019, pp.1107-1136. https://doi.org/10.1007/s11071-019-05252-7

[27] K Meidani, AP Hemmasian, S Mirjalili, A Barati Farimani, "Adaptive grey wolf optimizer," Neural Computing and Applications, vol.34, no.10, Sept.2022, pp. 7711-7731. https://doi.org/10.1007/s00521-021-06885-9

[28] I Sharma, V Kumar, S Sharma, "A comprehensive survey on grey wolf optimization," Recent Advances in Computer Science and Communications (Formerly: Recent Patents on Computer Science), vol.15, no.3, Sept.2022, pp.323-333. DOI: https://doi.org/10.2174/2666255813999201007165454

[29] X Zhang, Y Zhang, Z Ming, "Improved dynamic grey wolf optimizer," Frontiers of Information Technology & Electronic Engineering, vol.22, no.6, Sept.2021, pp.877-890. https://doi.org/10.1631/FITEE.2000191